Original Research

Histopathological changes in tear-secreting tissues and cornea in a mouse model of autoimmune disease

Masaya Hiraishi[1,*], Md Abdul Masum[1,2,*], Takashi Namba[1], Yuki Otani[1], Yaser HA Elewa[1,3], Osamu Ichii[1,4] and Yasuhiro Kon[1]

[1]Laboratory of Anatomy, Department of Basic Veterinary Sciences, Faculty of Veterinary Medicine, Hokkaido University, Sapporo 060-0618, Japan; [2]Department of Anatomy, Histology and Physiology, Faculty of Animal Science and Veterinary Medicine, Sher-e-Bangla Agricultural University, Dhaka 1207, Bangladesh; [3]Department of Histology, Faculty of Veterinary Medicine, Zagazig University, Zagazig 44519, Egypt; [4]Laboratory of Agrobiomedical Science, Faculty of Agriculture, Hokkaido University, Sapporo 060-8589, Japan
Corresponding author: Osamu Ichii. Email: ichi-o@vetmed.hokudai.ac.jp
*These authors contributed equally to this paper.

Impact statement

Cornea, an outermost layer of mammalian eye, is protected by tear film and abnormalities of tear film causes dry eye. Dry eye injures the cornea which results lower vision in patients. Several factors cause dry eye, including altered systemic conditions, environment, and immunological abnormality of the patient in autoimmune disease like Sjögren's syndrome (SS). However, the detailed pathology of autoimmune abnormality-mediated dry eye is unclear. Here we demonstrated that systemic autoimmune abnormality in BXSB-Yaa mice was associated with histological changes in the exocrine glands and cornea of the eyes. We also showed that BXSB-Yaa mice developed mild or early stage dry eye-like disease and explain the existence of a compensatory mechanism associated with the dysfunction of these tissues. Thus, BXSB-Yaa could be a model for SS-like disease-associated dry eye and these data would contribute to the understanding of the pathogenesis of autoimmune-related dry eye disease.

Abstract

The tear film covers the cornea, and its abnormalities (including immunological) induce dry eye. Using autoimmune disease model mice, BXSB/MpJ-*Yaa* (BXSB-Yaa), histopathological changes in the eye and tear-secreting tissues were examined using histopathology, immunohistochemistry, and electron microscopy at 8, 20, and 28 weeks for early, middle, and late disease stages. Early and middle stage BXSB-Yaa showed increased serum autoantibody and spleen weight-to-body weight (S/B) ratio, respectively, and higher tear volume than controls, BXSB/MpJ (BXSB), at early stages, which decreased with ageing and negatively correlated with autoimmune disease indices. Smaller Meibomian gland acini, intraorbital lacrimal glands, and Harderian gland acinar cells were seen in late stage BXSB-Yaa than in BXSB; the latter two indices decreased with ageing and negatively correlated with the S/B ratio. Cell infiltration occurred in the middle stage BXSB-Yaa extraorbital lacrimal gland, and acinar cells were smaller than BXSB. The conjunctival goblet cells decreased from early to middle stages in both strains, but in BXSB-Yaa, they increased at late stages with a partial lack of microvilli on the cornea and were inversely altered with anterior epithelium thickness through ageing, suggesting that they compensated for anterior epithelium damage. In conclusion, the tear film was unstable due to an autoimmune disease condition in BXSB-Yaa.

Keywords: Tear film, cornea, autoimmune disease, BXSB/MpJ-Yaa mice

***Experimental Biology and Medicine* 2020; 245: 999–1008. DOI: 10.1177/1535370220928275**

Introduction

For mammalian eyeballs, the outermost cornea is covered and protected by the tear film composed of mucin, water, and lipid layers from its inner side. Secretions from conjunctival goblet cells, lacrimal glands (LGs), and Meibomian glands (MG) contribute to the formation of the tear film.[1–3] The deep gland of the third eyelid, known as the Harderian gland (HG), also contributes to the formation of the lipid layer.[4] Dysfunction or injuries in these tear film-forming cells cause several eye diseases. Loss of conjunctival goblet cells and dysfunction of LGs as well as MGs cause disruption of the water layer, the efficient functioning of which is crucial in the prevention of water evaporation.[5–7] In general,

eye diseases due to tear film abnormalities are diagnosed as "dry eye" in humans and animals.

Dry eye injures the cornea in humans and companion animals; model animals of dry eye have been reported.[8–10] This disease reduces the quality of life in patients because it causes fatigue or pain of the eyes and eventually leads to low vision. Dry eye is known as a chronic disease associated with keratoconjunctivitis. Several factors cause dry eye, including altered systemic conditions, environment, ophthalmic operation, and an immune abnormality of the patient.[11–13] Sjögren's syndrome (SS), a representative autoimmune disease targeting exocrine glands, causes dry eye in humans.[14] Between 0.04 and 3.1 million adults suffer from SS in the United States.[15] While SS is not fatal, approximately 5% of patients with long-term SS develop malignant lymphoma.[16–18] Companion dogs that show dry eye associated with an autoimmune disorder have SS-like disease.[19,20] For dry eye in SS, autoimmune abnormality-associated inflammation in the LGs, MG dysfunction, and goblet cell loss is reported in human patients and model animals.[21–25] SS model mice have inflammation in the HG.[26] In Japan, SS is diagnosed in patients exhibiting more than two of the following characteristics: lymphocyte infiltration in labial salivary glands or LGs; hyposecretion of saliva; hyposecretion of tear fluid or an injured cornea; and anti-Ro/SS-A and anti-La/SS-B antibodies in the serum.

To elucidate the pathology of SS, the use of an animal model is crucial. The BXSB/MpJ-*Yaa* (BXSB-Yaa) mouse, carrying the Y-linked autoimmune accelerator (*Yaa*) mutation on the Y chromosome, is a representative autoimmune disease model and develops severe symptoms, including abnormal proliferation of B-cells, autoantibody production, splenomegaly, and glomerulonephritis.[27–29] BXSB-Yaa manifests SS-like symptoms, such as B-cell predominant lymphocytic infiltrations and the destruction of acini in extraorbital lacrimal glands (ELGs).[22] In that study, there was no significant difference in the quantity of tear production between BXSB-Yaa and healthy C57BL/6 mice, suggesting that BXSB-Yaa could be a model for mild or early stage dry eye. However, the detailed pathology of autoimmune abnormality-mediated dry eye is unclear since no study has elucidated the histopathological changes in tear-secreting tissues using SS model mice.

We investigated the histopathology of tear-secreting tissues and cornea in BXSB-Yaa mice, evaluating autoimmune disease development and tear production by comparing them to the healthy control strain BXSB/MpJ (BXSB). We found that BXSB-Yaa mice developed mild or early stage dry eye-like disease and discuss the existence of a compensatory mechanism associated with the dysfunction of these tissues in this model. These data contribute to the understanding of the pathogenesis of autoimmune-related dry eye disease.

Materials and methods

Animals

Male BXSB and BXSB-Yaa mice aged 8, 20, 24, and 28 weeks were purchased from Japan SLC, Inc. (Hamamatsu, Japan) and maintained under specific pathogen-free conditions. Animal experimentation was approved by the Institutional Animal Care and Use Committee of the Faculty of Veterinary Medicine, Hokkaido University (approval No. 16–0124). All experimental animals were handled in accordance with the Guide for the Care and Use of Laboratory Animals, Faculty of Veterinary Medicine, Hokkaido University (approved by the Association for Assessment and Accreditation of Laboratory Animal Care International).

Sample collection

Under deep anesthesia, using a mixture of medetomidine (0.3 mg/kg), midazolam (4 mg/kg), and butorphanol (5 mg/kg), tears were collected using Schirmer test paper (Schirmer Tear Production Measuring Strips; Showa Yakuhin, Tokyo, Japan), which was sliced at approximately 1 mm width and inserted into the lower conjunctival sac for 4 min. Then, blood was collected from the femoral arteries, and all mice were euthanized by cervical dislocation. The heads, eyeballs, periocular tissues, and spleens were immediately collected and used for further analysis.

Tear volume measurement

Tear volume was measured according to a previous report.[22] Briefly, using a digital image, the tear-wetted area of Schirmer test paper was measured using ImageJ (NIH, http://rsbweb.nih.govi/ij/) and estimated as the tear volume.

Serological analysis

Serum levels of anti-double-stranded DNA (dsDNA) antibody were measured to evaluate systemic autoimmune conditions and disease development using the LBIS Anti-dsDNA-Mouse ELISA Kit (FUIJIFILM Wako Pure Chemical Corporation; Osaka, Japan) according to the manufacturer's instructions.

Histopathological analysis

The eyeballs with conjunctiva, MG, and HG were fixed with 4% paraformaldehyde (PFA) at 4°C overnight. The tissues were dehydrated using alcohol and embedded in paraffin, cut into 3-μm-thick sections, and stained with hematoxylin-eosin (HE). Sections of the eyeball with conjunctiva were stained with periodic acid-Schiff (PAS). Skulls containing the intraorbital lacrimal gland (ILG) and ELG were first fixed with 4% PFA and then immersed in acetone overnight to eliminate lipids. Then, they were immersed in 10% formic acid for 12 h to decalcify. Paraffin sections (3-μm-thick) were prepared and stained with HE or PAS.

Histoplanimetry

HE-stained sections were converted to virtual slides using Nano Zoomer 2.0 RS (Hamamatsu Photonics Co., Ltd; Hamamatsu, Japan), and then each measurement was performed using NDP.view2 software (Hamamatsu Photonics Co., Ltd). The number of MG acini in the upper tarsal plates

in the defined area ($445 \times 352\,\mu m$) was counted for two areas and expressed as MG acinus density. For the HG, ELG, and ILG, the area of the acinus (1) and its ductal lumen (2) was measured by drawing a line on NDP.view2 (Hamamatsu Photonics Co., Ltd); the size of one acinus was obtained by subtracting (2) from (1). This measurement was performed randomly for 50 acini in the HG and ELG, and 30 acini in the ILG, for each sample. For the palpebral conjunctiva, goblet cell density in the conjunctiva epithelium was calculated from the number of goblet cells within the length of two non-overlapping areas from the upper and lower eyelids (more than 500 μm). We also measured the thickness of the anterior epithelium of the cornea at five points around the central part of the cornea.

Immunohistochemistry

Paraffin sections were deparaffinized and antigen retrieval was performed. The sections were soaked in methanol containing 0.3% H_2O_2 for 20 min at room temperature to remove internal peroxidase. After washing three times in phosphate-buffered saline (PBS), sections were incubated with blocking serum for 1 h at room temperature and primary antibodies overnight at 4°C. Prior to, and after sections were incubated with secondary antibodies for 30 min at room temperature, they were washed three times in PBS. The sections were incubated with streptavidin-conjugated horseradish peroxidase (SABPO (R) kit; Nichirei, Tokyo, Japan) for 30 min and washed three times in PBS. For visualization of the positive reactions, the sections were incubated with 10 mg 3, 3′-diaminobenzidine tetrahydrochloride in 50 mL 0.05 M Tris-HCl buffer-H_2O_2 solution. Finally, sections were stained with hematoxylin. Antibodies, antigen retrieval, and blocking details are listed in Supplementary Table 1.

Scanning electron microscopy

Whole eyeball samples from BXSB and BXSB-Yaa at 28 weeks of age were pre-fixed with 2.5% glutaraldehyde in 0.1 M phosphate buffer (PB) for 4 h at 4°C. Then, the samples were washed five times with 0.1 M PB for 10 min each. The samples were post-fixed with 1% OsO_4 for 1 h, immersed in 1% tannic acid solution (TAS) for 1.5 h as a conductive treatment, and washed six times with 0.1 M PB for 10 min each at 4°C. Then, the samples were post-fixed in 1% OsO_4 for 1 h again and washed again, as above. Subsequently, the samples were immersed in 0.5% TAS for 10 min and then 1.0% TAS for 1 h at 4°C. After washing in 0.1 M PB, the specimens were dehydrated with graded ethanol, replaced with isoamyl acetate, and dried using a critical point drier (HCP-2, Hitachi; Tokyo, Japan). The dried specimens were mounted on aluminium stubs, treated by ion sputtering (E-1030, Hitachi), and observed using an SEM (SU 8000, Hitachi; 10 kV).

Statistical analysis

The results are expressed as the mean ± standard error (SE). Analysis between two groups was conducted using the Mann–Whitney U test. Multiple comparisons over three groups were conducted using the Scheffé's method after the Kruskal–Wallis test. The correlation between two parameters was analyzed using Spearman's correlation test. In all analyses, $P < 0.05$ was regarded as significantly different.

Results

Autoimmune disease indices and tear volume

BXSB-Yaa mice at 8, 20, and 28 weeks of age were investigated as models of early, moderate, and late stage autoimmune disease, respectively. BXSB-Yaa showed significantly higher ratios of spleen weight-to-body weight (S/B) than BXSB at 20 weeks; BXSB-Yaa at 28 weeks showed significantly higher S/B than BXSB-Yaa at 8 weeks (Figure 1(a)). The serum levels of anti-dsDNA antibody were significantly higher in BXSB-Yaa than in BXSB at all examined weeks without age-related significant differences (Figure 1(b)). Although BXSB showed no significant age-related changes, tear volume in BXSB-Yaa decreased with age and showed a significant difference between 8 and 20 or 28 weeks (Figure 1(c)), and a significantly higher value than BXSB at 8 weeks.

Histopathology of the lipid layer-producing exocrine glands, MG, and HG

As shown in Figure 2(a), MGs were observed as a cluster of foamy sebaceous gland cells beneath the palpebral conjunctiva in the upper or lower tarsal plates. Melanin pigments were observed between the MG acini. No change in acinus morphology was observed among ages or strains, but the number of acini in BXSB-Yaa was lower than that in BXSB at all ages. The HG acini in the third eyelid were composed of clear glandular epithelial cells containing numerous minute lipids in their abundant cytoplasm (Figure 2(b)). Further, brown-colored porphyrins were observed in some acinar lumens. No change was observed in porphyrin appearance among ages or strains; acinus size decreased from 20 weeks in BXSB-Yaa, but not in BXSB. Inflammatory cell infiltrations in MG and HG were not obvious in all ages of both strains.

MG acinar density and HG acinar size in BXSB-Yaa were lower than those in BXSB at 8 and 20 weeks (Figure 2(c) and (d)); significant strain differences were detected at 28 weeks for both parameters. In BXSB-Yaa, HG values were significantly decreased from 8 weeks to 20 and 28 weeks (Figure 2(d)).

Histopathology of the water layer-producing exocrine glands, ELG, and ILG

Figure 3 shows the histopathological observation of LGs. For ELGs (Figure 3(a)), serous acini were composed of glandular epithelial cells with a clear and large cytoplasm in the apical portion and a basophilic one in the basal portion. The size of nuclei in acinar epithelial cells or acinar lumens differed among acini, but there was no consistent difference among ages or strains. Although the histological characteristics of ILG were similar to those of ELGs, the ILG

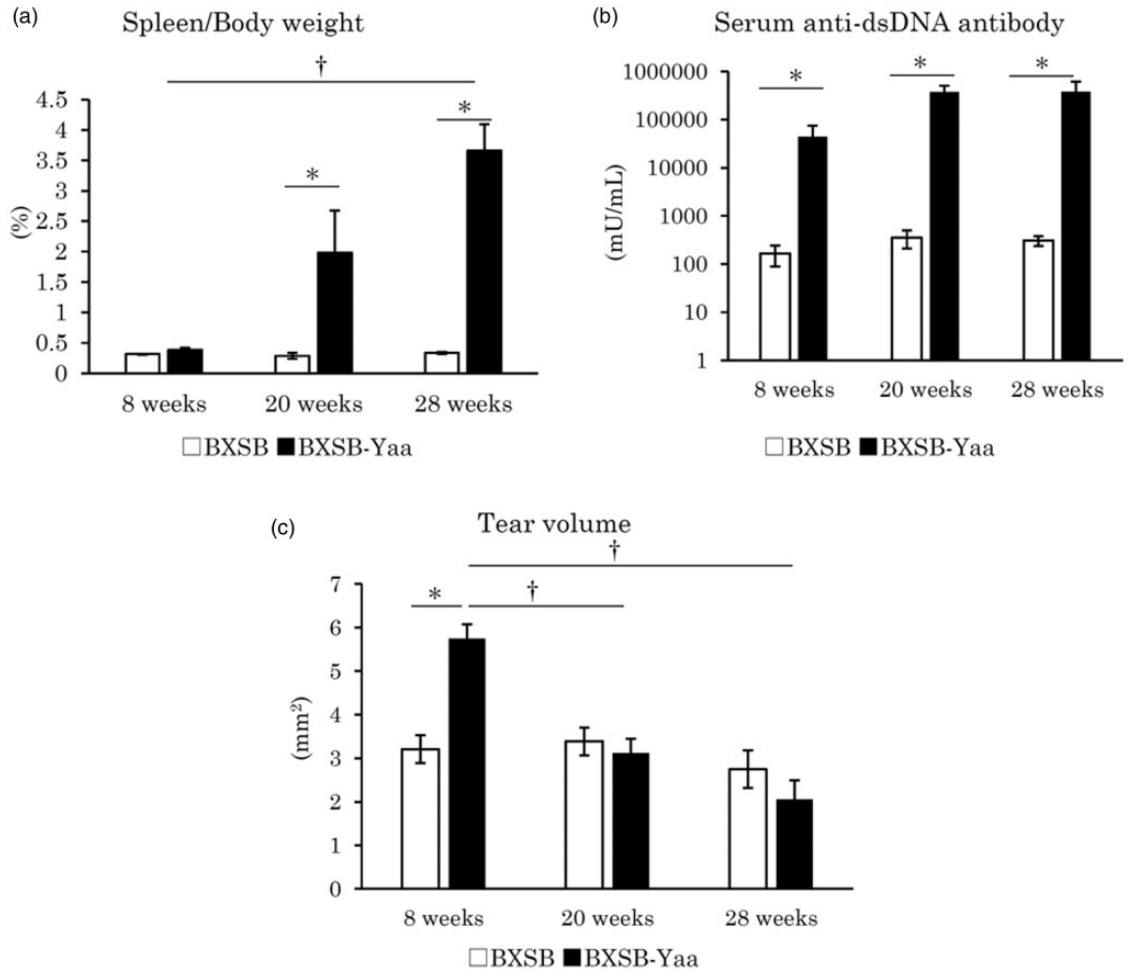

Figure 1. Indices for autoimmune abnormality and tear volume in mice. (a) The ratio of spleen weight-to-body weight. (b) The serum levels of anti-double stranded DNA (dsDNA) antibody. (c) Tear volume. BXSB: BXSB/MpJ. BXSB-Yaa: BXSB/MpJ-*Yaa*. Each bar represents the mean ± SE ($n = 4$). *Significant strain difference at the same age, Mann–Whitney U test. †**Significant** difference from the other groups, Kruskal–Wallis test followed by Scheffe's method.

acinus was smaller than that of ELG, and the ILG was separated into smaller lobules than the ELG (Figure 3(b)). No changes were observed in ELGs and ILGs of BXSB of all ages, but the acini in BXSB-Yaa at 20 and 28 weeks were smaller than those at 8 weeks.

ELG and ILG acinar sizes in BXSB-Yaa were lower than those in BXSB at 20 weeks, but the reduction in ELG acinar size was significant (Figure 3(c) and (d)). In BXSB, the ELG showed increased acinar sizes with age without statistical significance, but in BXSB-Yaa, ILG values significantly decreased from 8 weeks to 20 and 28 weeks (Figure 3(d)).

Since several mononuclear cells are observed between the acini of ELGs, particularly around the ducts, as shown in Figure 3(a) and previous reports,[17] cell infiltration was evaluated. In all samples, ELGs had cell infiltration at 8, 20, and 28 weeks in BXSB (0/4, 1/4, 2/4 animals, respectively) and BXSB-Yaa (0/4, 4/4, 4/4 animals, respectively). Using immunohistochemistry, these inflammatory cells comprised $B220^+$ B-cells, $CD3^+$ T-cells, and $Iba1^+$ macrophages (Figure 4(a) to (c)). For ILG, cell infiltration was scarce, but one sample from BXSB-Yaa at 20 weeks (1/4 animals) showed cell infiltration. These lesions comprised $B220^+$ B-cells, $CD3^+$ T-cells, and $Iba1^+$ macrophages, similar to ELG (Figure 4(d)).

Histopathology of mucin layer-producing goblet cells in the palpebral conjunctiva

In all mice, the palpebral or forniceal conjunctiva was composed of stratified cuboidal to columnar epithelium (Figure 5(a)). Several PAS-positive goblet cells were observed in the epithelium of the palpebral or forniceal conjunctiva. For the palpebral conjunctiva, there was no morphological difference between the upper and lower eyelids. In BXSB, the number of PAS^+ palpebral conjunctival goblet cells decreased at 20 and 28 weeks compared to those at 8 weeks. Goblet cell numbers also decreased in BXSB-Yaa from 8 to 20 weeks but increased again at 28 weeks. Figure 5(b) shows the goblet cell density in the palpebral conjunctiva. In BXSB-Yaa, PAS^+ conjunctival goblet cells significantly decreased from 8 to 20 weeks but increased from 20 to 28 weeks, without statistical significance. At 28 weeks, BXSB-Yaa showed significantly higher values than BXSB.

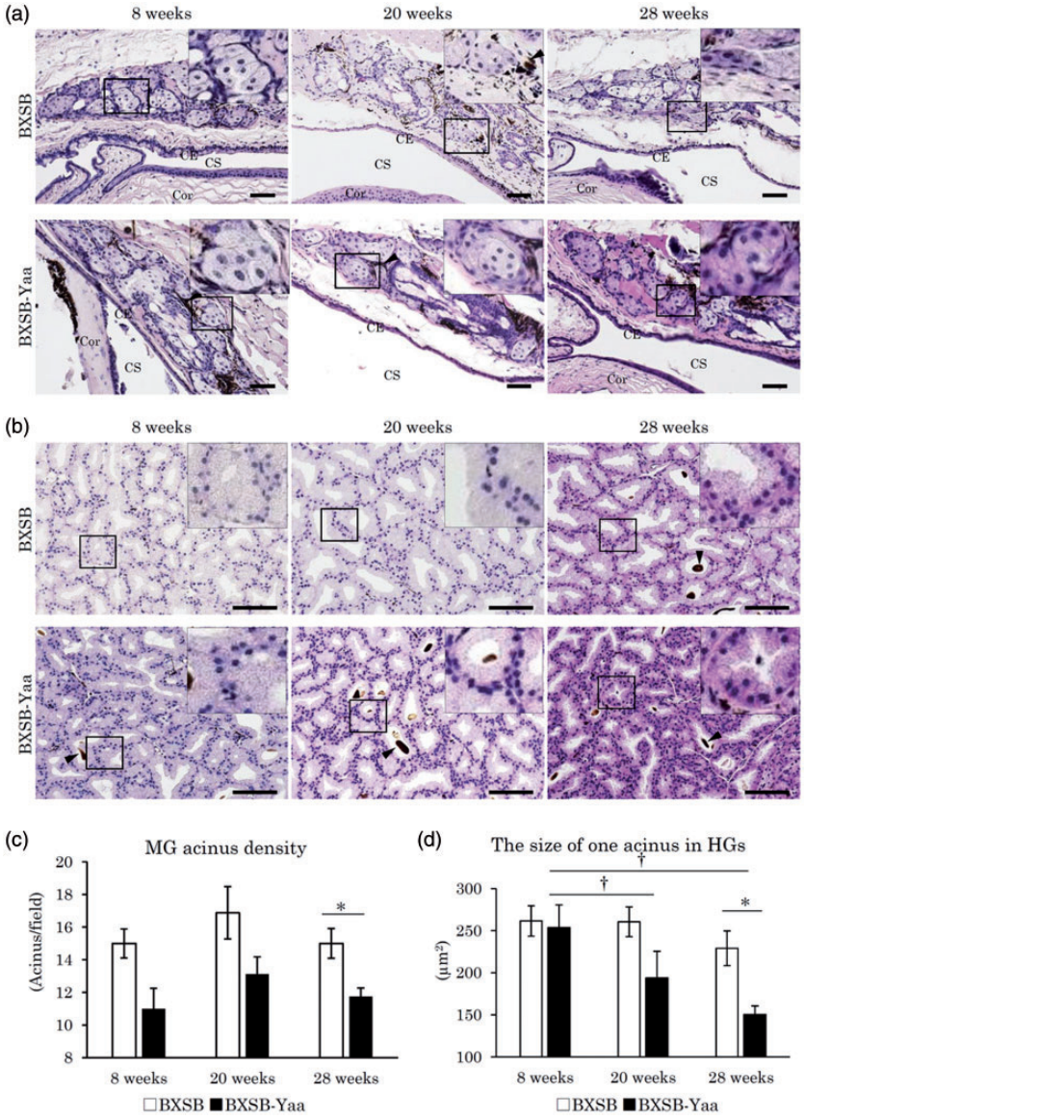

Figure 2. Histopathology of lipid layer-composing exocrine glands in mice. (a) Meibomian glands (MGs) in the upper tarsal plate. Sebaceous gland cells form clusters beneath the conjunctival epithelium (CE). Melanin pigments indicated by arrowheads are observed between and around acinar cells. CS: conjunctival sac; Cor: cornea. HE staining. Bars = 100 μm. (b) Harderian glands (HGs) in the third eyelid. Acini of HGs are composed of clear glandular epithelial cells containing numerous minute lipids in their abundant cytoplasm. Some acini include porphyrins in their lumens. Arrowheads point to porphyrin. Smaller acinar epithelial cells are observed in BXSB-Yaa at 20 and 28 weeks. HE staining. Bars = 100 μm. (c) MG acinus density. (d) The size of one acinus in HGs. BXSB: BXSB/MpJ. BXSB-Yaa: BXSB/MpJ-*Yaa* Each bar represents the mean ± SE ($n = 4$). *Significant strain difference at the same age, Mann–Whitney U test. †**Significant** difference from the other groups, Kruskal–Wallis test followed by the Scheffe's method. (A color version of this figure is available in the online journal.)

Histopathology of the cornea

The cornea is composed of the anterior epithelium, the proper substance, the posterior limiting membrane (Descemet's membrane), and the posterior epithelium from the outside, as shown in Figure 6(a). The anterior epithelium is stratified squamous epithelium with five to seven cell layers, which is influenced by changes in the tear film,[30] and it thickened with ageing in BXSB, but not in BXSB-Yaa (Figure 6(a)). BXSB, but not BXSB-Yaa, had significantly increased thickness of the anterior corneal epithelium from 8 weeks to 20 weeks, but the epithelium in BXSB-Yaa was significantly thinner than that in BXSB at 28 weeks (Figure 6(b)).

SEM analysis of the ultrastructure of the corneal surface was performed in BXSB and BXSB-Yaa at 28 weeks (Figure 6 (c)). Under low magnification, BXSB showed a smooth and flat surface, whereas BXSB-Yaa showed a few dark areas. Under high magnification, the surface of the cornea was covered by numerous microvilli in BXSB, but the dark area, observed under low magnification, lacked intact microvilli in 75% of the examined BXSB-Yaa ($n = 4$).

Correlation between tear volume, autoimmune disease indices, and altered tear-secreting tissue morphologies

The correlations among tear volumes, the indices of autoimmune disease, and tear-secreting tissue morphologies

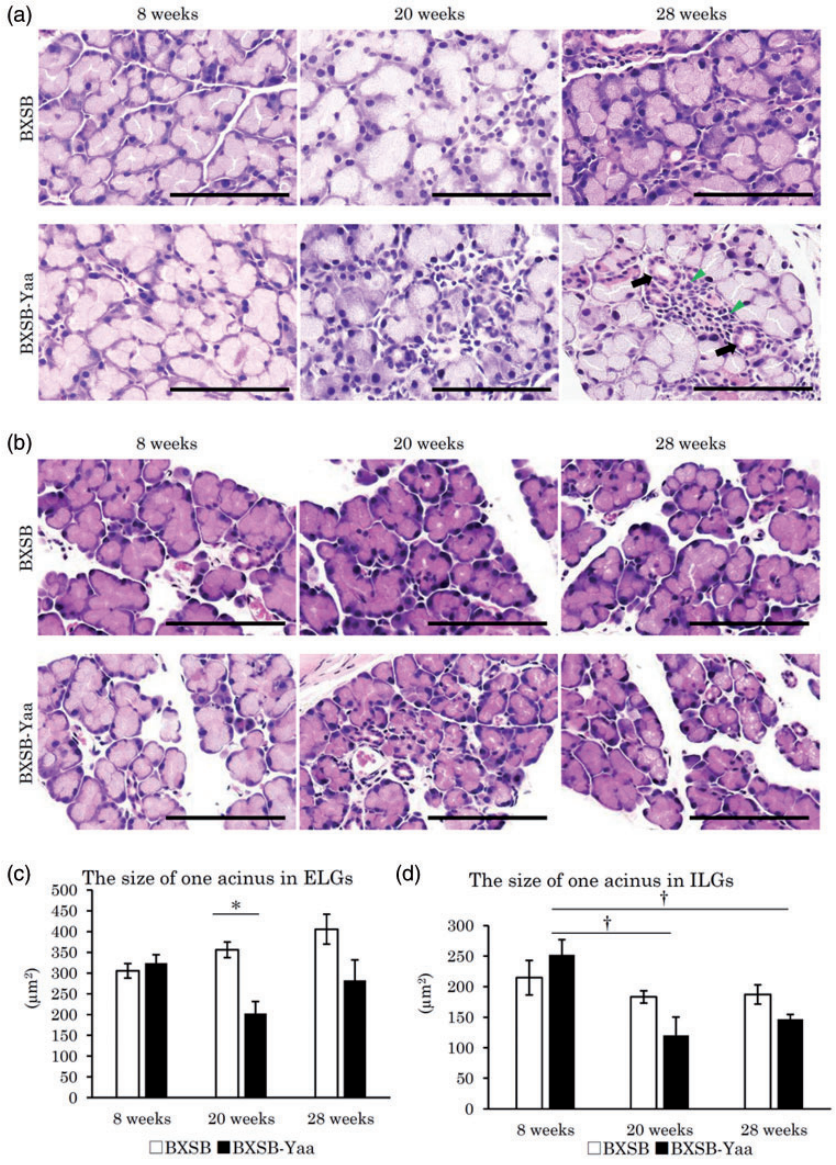

Figure 3. Histopathology of water layer-composing exocrine glands in mice. (a) Extraorbital lacrimal glands (ELGs). Each acinus is composed of serous cells and a small lumen. Mononuclear cells (arrowheads) are observed around the ducts (arrows). Smaller acini are observed in BXSB-Yaa at 20 and 28 weeks. HE staining. Bars = 100 μm. (b) Intraorbital lacrimal glands (ILGs). Histological characteristics are similar to those of ELG. These glands are separated into smaller lobules. Smaller acini are observed in BXSB-Yaa at 20 and 28 weeks. HE staining. Bars = 100 μm. (c) Size of one acinus in ELGs. (d) Size of one acinus in ILGs. BXSB: BXSB/MpJ. BXSB-Yaa: BXSB/MpJ-*Yaa* Each bar represents the mean ± SE ($n = 4$). *Significant strain difference at the same age, Mann–Whitney U test. †**Significant** from the other groups, Kruskal–Wallis test followed by the Scheffe's method. (A color version of this figure is available in the online journal.)

are summarized in Table 1. For all mice, tear volume showed no correlations with any parameters, but S/B and anti-dsDNA antibody were significantly and negatively correlated with MG and HG histological parameters. S/B also correlated with ELG and ILGs, indicating the relationship between autoimmune disease development and histopathological alterations.

BXSB-Yaa tear volume was significantly and positively correlated with ILG histological parameters, and S/B significantly and negatively correlated with HG and ILG histological parameters, as well as tear volume, showing age-related decreases in this strain. This result correlates autoimmune disease progression with alteration of tear volume and morphological changes in these organs. Moreover, our correlation analysis revealed that corneal histopathological parameters were only significantly and negatively correlated with conjunctival goblet cells in all mice and BXSB-Yaa mice (Supplemental Table 1).

Discussion

BXSB-Yaa showed increased serum levels of anti-dsDNA antibody and S/B from 8 to 20 weeks, indicating the onset of autoimmune abnormality started from 8 weeks. Although the tear volume index decreased with age in BXSB-Yaa, these mice showed higher values than BXSB at eight weeks. The Schirmer test paper indicated basal as well as reflex secretion of tears due to the physical stimuli of paper insertion into the conjunctival sac.[21] Therefore, the altered tear volume in BXSB-Yaa suggested a change in

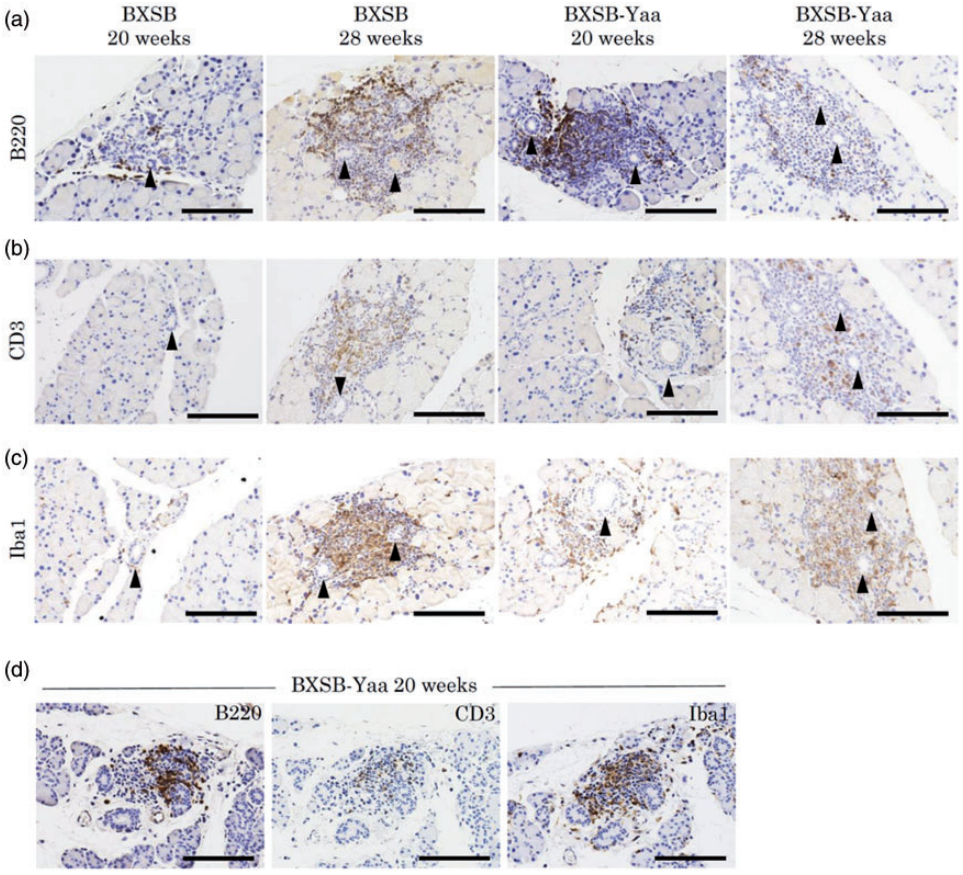

Figure 4. Inflammatory cell infiltration in lacrimal glands. (a–c) Immunohistochemistry for B220 (panel A), CD3 (panel B), and Iba1 (panel C) in extraorbital lacrimal glands. Positive cells localize around the ducts (arrowheads). Bars = 100 μm. (d) Immunohistochemistry for B220, CD3, and Iba1 in intraorbital lacrimal glands in BXSB-Yaa at 20 weeks of age. Bars = 100 μm. (A color version of this figure is available in the online journal.)

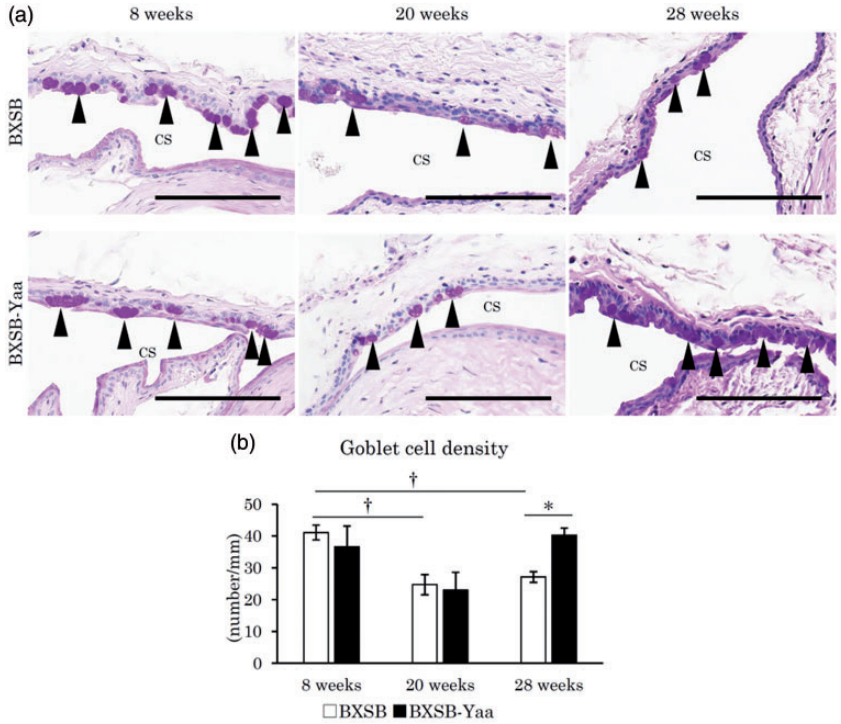

Figure 5. Histopathology of mucin layer-producing tissues in mice. (a) Palpebral conjunctiva in the upper or lower eyelids. PAS^{+} goblet cells, indicated by arrowheads, are observed in the epithelium of the palpebral conjunctiva. The number of goblet cells decreased in BXSB with age, but not in BXSB-Yaa. PAS staining. Bars = 100 μm. CS: conjunctival sac. (b) Goblet cell density in the conjunctival epithelium. BXSB: BXSB/MpJ. BXSB-Yaa: BXSB/MpJ-*Yaa* Each bar represents the mean ± SE ($n = 4$). *Significant strain difference at the same age, Mann–Whitney U test. †**Significant** difference from the other groups, Kruskal–Wallis test followed by the Scheffe's method. (A color version of this figure is available in the online journal.)

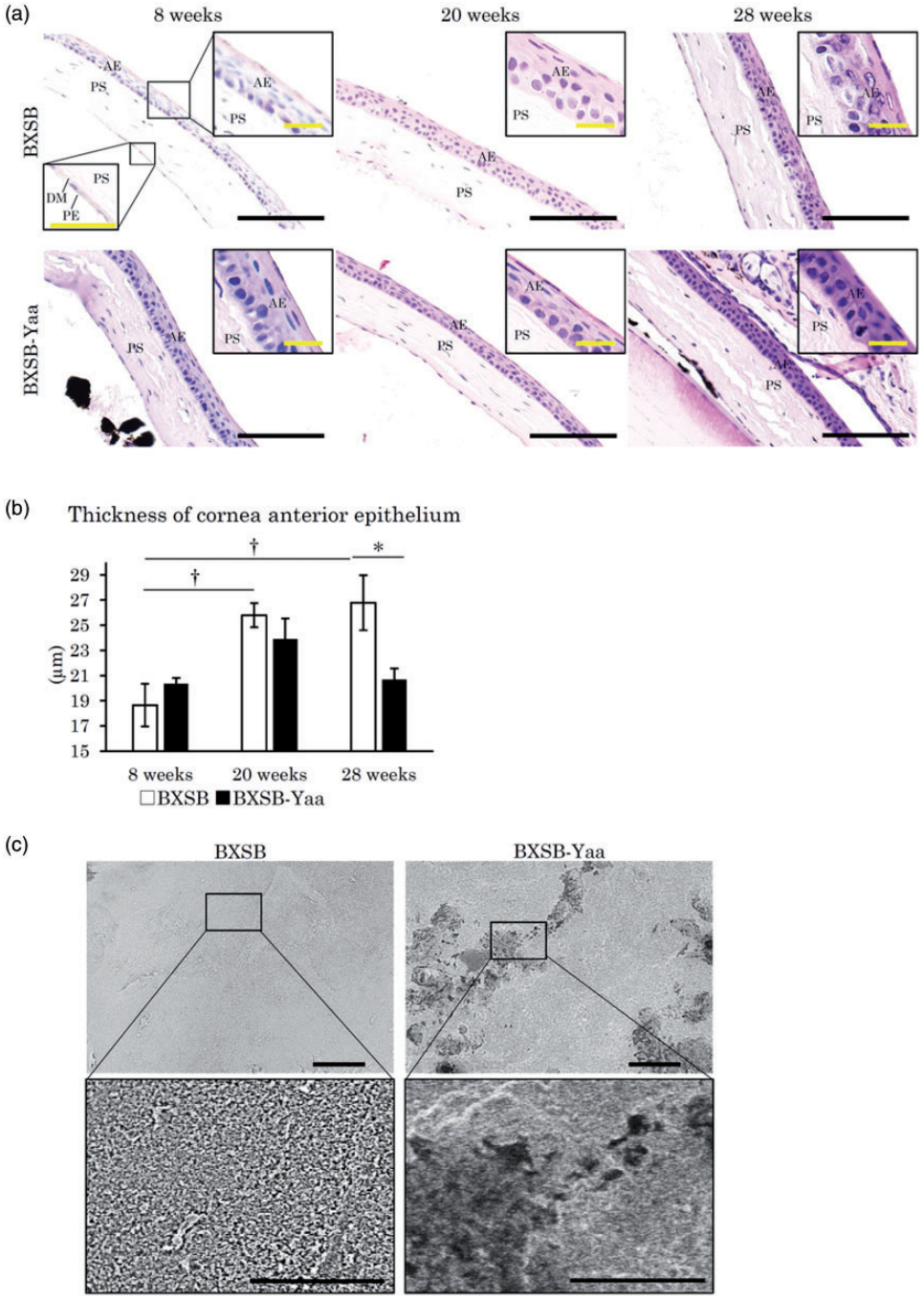

Figure 6. Histopathology of cornea in mice. (a) Cornea histology. The cornea is composed of four layers: the anterior epithelium (AE), the proper substance (PS), Descemet's membrane (DM), and the posterior epithelium (PE). The anterior epithelia of the cornea thickened with age in BXSB, but not in BXSB-Yaa. HE staining. Bars (black) = 100 μm. Bars (inset) = 20 μm. (b) Thickness of corneal AE. (c) Scanning electron microscopy images of the anterior surface of the cornea. Numerous microvilli cover the surface of the cornea in BXSB, and they disappear in some areas in BXSB-Yaa at 28 weeks of age. The area without microvilli is surrounded by a dotted line. Bars = 5 μm. BXSB: BXSB/MpJ. BXSB-Yaa: BXSB/MpJ-*Yaa* Each bar represents the mean ± SE ($n = 4$). *Significant strain difference at the same age, Mann–Whitney U test. †**Significant** difference from the other groups, Kruskal–Wallis test followed by the Scheffe's method. (A color version of this figure is available in the online journal.)

basal and/or reflex secretion from tear-producing components. At eight weeks, there was no significant difference in the tear film- or cornea-associated histoplanimetry between the two strains, but BXSB-Yaa showed a lower MG acinar density, an important component forming the tear film lipid layer. Tear volume increases to compensate for the decreased lipid layer in stearoyl coenzyme A desaturase-1 (SCD-1) deficient mice, which lack the enzyme related to lipid synthesis and suffer from MG dysfunction.[31] Tear volume and autoimmune indices were significantly and negatively correlated in BXSB-Yaa. Thus, we hypothesized that tear volume increased to compensate for the decreased lipid layer from MG dysfunction in young BXSB-Yaa and decreased with the progression of autoimmune disease and the altered function of tear film-producing organs.

Table 1. Correlations among tear volume, autoimmune disease indices, and altered tear-secreting tissue morphologies.

				Lipid		Water		Mucin	
			Tear volume	MG	HG	ELG	ILG	Conjunctiva	Cornea
All	Tear volume	ρ	1.000	−0.219	0.161	–0.009	0.323	–0.050	0.015
		P	–	0.304	0.453	0.968	0.124	0.816	0.944
	S/B	ρ	−0.184	−0.481*	−0.591**	−0.418*	−0.475*	0.176	−0.157
		P	0.391	0.017	0.002	0.042	0.019	0.412	0.465
	Anti-dsDNA antibody	ρ	−0.085	−0.619**	−0.436*	−0.388	−0.286	−0.109	−0.117
		P	0.694	0.001	0.033	0.061	0.175	0.612	0.588
BXSB-Yaa	Tear volume	ρ	1.000	−0.360	0.455	0.161	0.587*	−0.098	−0.077
		P	–	0.25	0.138	0.618	0.045	0.762	0.812
	S/B	ρ	−0.930**	0.322	−0.664*	−0.315	−0.608*	0.119	0.182
		P	0	0.308	0.018	0.319	0.036	0.713	0.572
	Anti-dsDNA antibody	ρ	−0.657*	0.265	−0.126	−0.224	−0.545	−0.420	0.420
		P	0.02	0.405	0.697	0.484	0.067	0.175	0.175

Note: Spearman's rank correlation coefficients $^*P < 0.05$, $^{**}P < 0.01$.
All mice ($n = 24$), BXSB-Yaa: **BXSB/MpJ-*Yaa*** ($n = 12$).
S/B: the ratio of spleen weight to body weight; Tear: tear volume; MG: MG acinus density; HG: the size of one acinus in the Harderian gland; ELG: the size of one acinus in the extraorbital lacrimal gland; ILG: the size of one acinus in the intraorbital lacrimal gland; conjunctiva: the goblet cell density in the conjunctiva epithelium; cornea: the thickness of the corneal anterior epithelium; -: not determined.

In aged BXSB-Yaa (middle and late stage), altered acinar morphology was observed in ELG and ILG, the water layer-producing components. Cell infiltration in these LGs was observed in BXSB-Yaa but not in BXSB. The destruction of LGs and salivary glands in SS model mice is mediated by cytokines, such as interleukins or interferons, secreted from infiltrating lymphocytes.[32] In BXSB-Yaa, the histological changes in ILG, but not in ELG, significantly correlated with tear volume and S/B, suggesting a close relationship between altered ILG morphology and autoimmune disease or tear production in mice, although ELGs showed more cell infiltration than ILGs. Only the LGs showed obvious inflammatory features, even though HG and MG morphologies were altered in ageing BXSB-Yaa. Thus, lipid- and water layer-producing organs showed different pathological processes; however, further study is needed to elucidate the mechanisms. Moreover, clarification of the cellular cluster around the duct as a tertiary lymphoid cluster might prove valuable to identify the mechanisms of the histomorphological changes of LG.

Age-related changes in HG, ELG, ILG, and conjunctiva goblet cell histopathological indices in BXSB-Yaa at 20 weeks indicated their altered morpho-function, assuming they were associated with tear film stability. While the anterior corneal epithelium thickened from 8 to 20 weeks in both strains, it was thinner in BXSB-Yaa than in BXSB at 28 weeks. Consistent with our results, the anterior corneal epithelium thickens with ageing in healthy mice,[33] and dry eye model mice have thinner corneal epithelium due to cell injuries than healthy controls.[10] A previous study showed that tear film instability could cause potential damage to the ocular surface.[30] Our SEM data also revealed that several areas on the corneal surface lacked microvilli in aged-BXSB-Yaa, which might reflect corneal injury at 28 weeks due to the unstable tear film.

The density of conjunctival goblet cells and mucin layer-associated cells decreased after 20 weeks in BXSB. Conjunctival goblet cell density decreases in healthy mice with ageing.[34] Cell density in BXSB-Yaa decreased from 8 to 20 weeks but recovered at 28 weeks. At 28 weeks, the BXSB-Yaa group developed prominent autoimmune disease abnormalities that significantly altered the tear film-producing organs, including MG, HG, ILG, and the cornea. Moreover, inflammatory cytokines associated with SS contribute to dry eye by inducing apoptosis and increasing mucin secretion and conjunctival goblet cell proliferation.[35] Therefore, we hypothesized that increased goblet cells in BXSB-Yaa at 28 weeks compensated for their altered morpho-function. In fact, SCD-1 deficient mice, which exhibit MG dysfunction, show a compensatory increase in mucin levels in their tears.[31] Our correlation analysis revealed that conjunctival goblet cells and corneal histopathological parameters showed significant and negative correlations in all mice ($\rho = -0.685$, $P < 0.01$) and BXSB-Yaa ($\rho = -0.748$, $P < 0.01$), supporting this compensation theory.

Here, BXSB-Yaa satisfied at least two of the Japanese SS diagnostic criteria: lymphocytic infiltration in LGs and corneal injury. Therefore, BXSB-Yaa could be a model for SS-like disease, even if lacrimal hyposecretion did not develop. SS-like disease in model mice progresses according to three phases.[36] Phase 1 shows increased apoptosis of acinar cells and abnormal protein or gene expression. Phase 2 shows inflammatory cell infiltration into the exocrine gland and autoantibody production. Phase 3 shows loss of secretory function progression, as found in dry eye. Based on this study, and another,[22] BXSB-Yaa developed phase 2 SS. This autoimmune disease-prone strain would likely develop dry eye because tear volume significantly decreases with ageing in these mice.

In conclusion, we demonstrated that systemic autoimmune abnormality in BXSB-Yaa was associated with histological changes in the exocrine glands and cornea of the eyes. Thus, BXSB-Yaa could be a model for mild stage SS-like disease-associated dry eye. Further studies focusing on the cause of morphological or detailed functional changes in tear-secreting glands would elucidate the pathology of SS-associated symptoms in human and veterinary medicine.

Authors' contributions

MH, MAM, TN, YO, YHAE, OI, and YK designed and performed experiments. MH and MAM analyzed the data. All authors were involved in writing the paper and approved the final manuscript.

ACKNOWLEDGEMENT

This research was awarded the Encouragement Award (undergraduate section) at the 162nd Japanese Association of Veterinary Anatomists in Tsukuba, Japan (September 2019).

DECLARATION OF CONFLICTING INTERESTS

The author(s) declared no potential of interest with respect to the research, authorship, and/or publication of this article.

FUNDING

The author(s) received no financial support for the research, authorship, and/or publication of this article.

ORCID iD

Md Abdul Masum https://orcid.org/0000-0003-3049-3777

SUPPLEMENTAL MATERIAL

Supplemental material for this article is available online.

REFERENCES

1. Walcott B. The lacrimal gland and its veil of tears. *News Physiol Sci* 1998;**13**:97–103
2. Shinomiya K, Ueta M, Kinoshita S. A new dry eye mouse model produced by exorbital and intraorbital lacrimal gland excision. *Sci Rep* 2018;**8**:1483
3. Foulks GN, Bron AJ. Meibomian gland dysfunction: a clinical scheme for description, diagnosis, classification, and grading. *Ocul Surf* 2003;**1**:107–26
4. Payne AP. The Harderian gland: a tercentennial review. *J Anat* 1994;**185**:1–49
5. Barbosa FL, Xiao Y, Bian F, Coursey TG, Ko BY, Clevers H, de Paiva CS, Pflugfelder SC. Goblet cells contribute to ocular surface immune tolerance-implications for dry eye disease. *Int J Mol Sci* 2017;**18**:E978
6. Ralph RA. Conjunctival goblet cell density in normal subjects and in dry eye syndromes. *Invest Ophthalmol* 1975;**14**:299–302
7. Mishima S, Maurice DM. The oily layer of the tear film and evaporation from the corneal surface. *Exp Eye Res* 1961;**1**:39–45
8. Cui X, Hong J, Wang F, Deng SX, Yang Y, Zhu X, Wu D, Zhao Y, Xu J. Assessment of corneal epithelial thickness in dry eye patients. *Optom Vis Sci* 2014;**91**:1446–54
9. Dodi PL. Immune-mediated keratoconjunctivitis sicca in dogs: current perspectives on management. *Vet Med* 2015;**6**:341–7
10. Marques DL, Alves M, Modulo CM, da Silva L, Reinach P, Rocha EM. Lacrimal osmolaritu and ocular surface in experimental model of dry eye caused by toxicity. *Rev Bras Oftalmol* 2015;**74**:68–72
11. Alves M, Novaes P, MdeA M, Reinach P, Rocha EM. Is dry eye an environmental disease? *Arq Bras Oftalmol* 2014;**77**:193–200
12. Stevenson W, Chauhan SK, Dana R. Dry eye disease: an immune-mediated ocular surface disorder. *Arch Ophthalmol* 2012;**130**:90–100
13. Toda I. Dry eye after lasik. *Invest Ophthalmol Vis Sci* 2018;**59**:109–15
14. Sjogren H. Keratoconjunctivitis sicca and chronic polyarthritis. *Acta Med Scand* 1948;**130**:484–8
15. Helmick CG, Felson DT, Lawrence RC, Gabriel S, Hirsch R, Kwoh CK, Liang MH, Kremers HM, Mayes MD, Merkel PA, Pillemer SR, Reveille JD, Stone JH. Estimates of the prevalence of arthritis and other rheumatic conditions in the United States. *Arthritis Rheum* 2008;**58**:15–25
16. Ambrosetti A, Zanotti R, Pattaro C, Lenzi L, Chilosi M, Caramaschi P, Arcaini L, Pasini F, Biasi D, Orlandi E, D'Adda M, Lucioni M, Pizzolo G. Most cases of primary salivary mucosa-associated lymphoid tissue lymphoma are associated either with sjoegren syndrome or hepatitis C virus infection. *Br J Haematol* 2004;**126**:43–9
17. de Vita S, Boiocchi M, Sorrentino D, Carbone A, Avellini C, Dolcetti R, Marzotto A, Gloghini A, Bartoli E, Beltrami CA, Ferraccioli G. Characterization of prelymphomatous stages of B cell lymphoproliferation in Sjogren's syndrome. *Arthritis Rheum* 1997;**40**:318–31
18. Voulgarelis M, Moutsopooulos HM. Lymphoproliferation in autoimmunity and Sjögren's syndrome. *Curr Rheumatol Rep* 2003;**5**:317–23
19. Nabeta R, Kambe N, Nakagawa Y, Chiba S, Xiantao H, Furuya T, Kishimoto M, Uchide T. Sjögren's-like syndrome in a dog. *J Vet Med Sci* 2019;**81**:886–9
20. Quimby FW, Schwartz RS, Poskitt T, Lewis RM. A disorder of dogs resembling Sjögren's syndrome. *Clin Immunol Immunopathol* 1979;**12**:471–6
21. Kosenda K, Ichii O, Otsuka S, Hashimoto Y, Kon Y. BXSB/MpJ-Yaa mice develop autoimmune dacryoadenitis with the appearance of inflammatory cell marker messenger RNAs in the lacrimal fluid. *Clin Experiment Ophthalmol* 2013;**41**:788–97
22. Hoffman RW, Alspaugh MA, Waggie KS, Durham JB, Walker SE. Sjögren's syndrome in MRL/l and MRL/n mice. *Arthritis Rheum* 1984;**27**:157–65
23. Sullivan DA, Dana R, Sullivan RM, Krenzer KL, Sahin A, Arica B, Liu Y, Kam WR, Papas AS, Cermak JM. Meibomian gland dysfunction in primary and secondary Sjögren syndrome. *Ophthalmic Res* 2018;**59**:193–205
24. Wang C, Zaheer M, Bian F, Quach D, Swennes AG, Britton RA, Pflugfelder SC, de Paiva CS. Sjögren-like lacrimal keratoconjunctivitis in germ-free mice. *Int J Mol Sci* 2018;**19**:pii:E565
25. Williamson J, Gibson AA, Wilson T, Forrester JV, Whaley K, Dick WC. Histology of the lacrimal gland in keratoconjunctivitis sicca. *Br J Ophthalmol* 1973;**57**:852–8
26. Jabs DA, Alexander EL, Green WR. Ocular inflammation in autoimmune MRL/Mp mice. *Invest Ophthalmol Vis Sci* 1985;**26**:1223–9
27. Haywood MEK, Rogers NJ, Rose SJ, Boyle J, McDermott A, Rankin JM, Thiruudaian V, Lewis MR, Fossati-Jimack L, Izui S, Walport MJ, Morley BJ. Dissection of BXSB lupus phenotype using mice congenic for chromosome 1 demonstrates that separate intervals direct different aspects of disease. *J Immunol* 2004;**173**:4277–85
28. Kimura J, Ichii O, Otsuka S, Sasaki H, Hashimoto Y, Kon Y. Close relations between podocyte injuries and membranous proliferative glomerulonephritis in autoimmune murine models. *Am J Nephrol* 2013;**38**:27–38
29. Pisitkun P, Deane JA, Difilippantonio MJ, Tarasenko T, Satterthwaite AB, Balland S. Autoreactive B cell responses to RNA-related antigens due to TLR7 gene duplication. *Science* 2006;**312**:1669–72
30. Lam H, Bleiden L, de Paiva CS, Farley W, Stern ME, Pflugfelder SC. Tear cytokine profiles in dysfunctional tear syndrome. *Am J Ophthalmol* 2009;**147**:198–205
31. Inaba T, Tanaka Y, Tamaki S, Ito T, Ntambi JM, Tsubota K. Compensatory increases in tear volume and mucin levels associated with meibomian gland dysfunction caused by stearoyl-CoA desaturase-1 deficiency. *Sci Rep* 2018;**8**:3358
32. Hayashi T. Dysfunction of lacrimal and salivary glands in sjögren's syndrome: nonimmunologic injury in preinflammatory phase and mouse model. *J Biomed Biotechnol* 2011;**2011**:407031
33. Inomata T, Mashaghi A, Hong J, Nakao T, Dana R. Scaling and maintenance of corneal thickness during aging. *PLoS One* 2017;**12**:e0185694
34. Volpe EA, Henriksson JT, Wang C, Barbosa FL, Zaheer M, Zhang X, Pflugfelder SC, de Paiva CS. Interferon-gamma deficiency protects against aging-related goblet cell loss. *Oncotarget* 2016;**7**:64605–14
35. Contreras-Ruiz L, Ghosh-Mitra A, Shatos MA, Dartt DA, Masli S. Modulation of conjunctival goblet cell function by inflammatory cytokines. *Mediators Inamm* 2013;**2013**:636812
36. Lee BH, Tudares MA, Nguyen CQ. Sjögren's syndrome: an old tale with a new twist. *Arch Immunol Ther Exp* 2009;**57**:57–66

(Received March 13, 2020, Accepted April 28, 2020)